Research Article
doi: 10.1590/01047760202330013338
vol(30), 2024

CERNE

Effects of flight and smoothing parameters of number of trees with aerial imagery in a native Brazilian atlantic forest remnant

Carla Talita Pertille[1]✤, Karla Mayara Almada Gomes[1], Darcy Maria da Conceição Laura dos Santos[1], Hudson Franklin Pessoa Veras[2], Midhun Mohan[3], Carlos Roberto Sanquetta[1], Alexandre Behling[1], Ana Paula Dalla Corte[1]

[1]Federal University of Paraná, Brazil
[2]Federal Institute of Acre, Brazil
[3]University of California, USA

FOREST MANAGEMENT

ABSTRACT

Background: The objective of this study was to detect native trees from different flight configurations and smoothing techniques in Canopy Height Models (CHMs) in a native remnant in the municipality of Curitiba, State of Paraná, Brazil. To do so, eight flights were carried out with a Phantom 4, with two flight planning applications (Litchi and Pix4Dcapture) and two flight arrangements (single and double), totaling four flights for each application. All flights were processed using the Pix4Dmapper program. The LiDAR database was obtained with a DJI Matrice 300 system and from this data, the Digital Terrain Model (DTM) of the area was extracted. From the UAV data, the Digital Surface Model (DSM) of each flight was obtained. Subtracting each DSM from the DTM resulted in the CHMs for each UAV flight flown. The CHMs were smoothed with the CHMsmoothing function and three search window sizes were tested (6.5 x 6.5, 8 x 8, and 10 x 10).

Results: The results of the ITD approach revealed that in unsmoothed and smoothed CHMs, the search window of size 8 resulted in the best precision metrics, with the highest recall, precision, and F-score values. In the smallest window size, there was the highest number of false positives while in the largest window size, the omitted trees were more representative.

Conclusion: The best combination between flight parameters and smoothing techniques was with the Litchi application, with a single flight and 80% lateral and longitudinal overlap, resulting in individuals detected with an F-score of 0.94.

Keywords: Remote sensing; LM algorithm; canopy height model.

HIGHLIGHTS

The lateral and longitudinal overlap evaluated as well as the applications tested did not differ in terms of the number of trees detected.
Flights with a double design showed greater drag in the images generated.
In the tested algorithm, the smaller search window size resulted in more falsely detected trees and the larger search window size caused greater omission of individuals.
The simple flight with 80% lateral and longitudinal overlap detected trees with an F-score of 0.94.

PERTILLE, C. T.; GOMES, K. M. A.; SANTOS, D. M. C. L.; VERAS, H. F. P.; MOHAN, M.; SANQUETTA , C. R.; BEHLING, A.; CORTE, A. P. D. Effects of flight and smoothing parameters of number of trees with aerial imagery in a native Brazilian atlantic forest remnant. CERNE, v.30, e-103338, doi: 10.1590/01047760202430013338.

✤Corresponding author: carla.pertille@ufpr.br
Received: October 2/2023 Accepted: May 18/2024

Open Access
CERNE
ISSN 0104-7760
UFLA UNIVERSIDADE FEDERAL DE LAVRAS

INTRODUCTION

Native forests offer indispensable ecosystem services to the society, making it necessary to understand the patterns of these environments for conservation of the remaining resources. However, obtaining large-scale and accurate data to assess the heterogeneous structure of natural forest ecosystems in the field is a complex task (Fraser and Congalton, 2018). An alternative way to this is the use of modern tools, including proximate and remote sensing data that can assimilate large amounts of data which can then have transformed them into useful information to support conservation strategies and sustainable use of forest resources (Fraser and Congalton, 2018).

Data in forest inventories are generally collected from field measurements that can be costly and with a degree of complexity to perform, particularly in complex native forests which may also be less accessible than plantation forests, depending on the vegetation density, slope of the areas, climatic factors (rain, wind, etc.), vegetation characteristics and availability of appropriate equipment. Efficient methodologies and/or tool for forest inventories in native remain sparse. In this context, Mohsan et al. (2022) and Fassnacht et al. (2023) suggest the use of Remote Sensing (RS) techniques as a reliable and efficient option for carrying out traditional forestry measurements.

The growing evolution of RS in the 21st century favored expanding the scales at which spatial data are collected by the creation of new sensors and sensor platforms such as Unmanned Aerial Vehicles (UAVs) (Fraser and Congalton, 2018). It is noteworthy that expressive advances of sensors implanted in UAVs created a new generation of services, especially Individual Tree Detection (ITD) allowing the protection of forest structural attributes such as tree height, crown width, diameter at breast height (DBH), biomass and forest uniformity (Millikan et al., 2019; Mohan et al., 2017; Jaafar et al., 2018; Yu et al., 2022; Ottoy et al., 2022).

Delimiting tree canopies allows assessing forest status and density. However, this mapping becomes costly with traditional field techniques (Tang and Shao, 2015), highlighting the importance of developing accurate and efficient survey techniques for tree detection, in addition to classical and deep learning methods.

Therefore, there is a gap in the selection of the accuracy algorithm for tree detection, especially regarding factors related to UAV image acquisition and the subsequent generation of its products, such as digital models. Knowing that studies with aerial images in forest areas present different parameters according to their applications, the influence of factors such as focal length, camera vertical angle, height, speed, flight route and aircraft orientation must be evaluated (Nevalainen et al., 2017) on the quality of the Canopy Height Model (CHM) and consequently, on the accuracy of the trees detected from different techniques. These parameters are important because overlaps determine the number of varied viewing angles of a given object within the scene, as well as the degree of redundancy between images (Iglhault et al., 2019), the type of flight (single or double) directly influences the duration of the flight, and consequently the battery and the application for executing the flight manages the flight plan and is responsible for controlling the aircraft.

Inserted in this theme, this objective is based on the hypothesis that flight parameters can contribute to enhancing the quality of generated products, such as CHM, and consequently, in the individual detection of trees. That said, the objective of this study was to develop a proposal for the optimal determination of aerophotogrammetric flight parameters (i.e., image overlap, flight design and flight app) for generating digital surfaces for the detection species trees with ITD approach in a native Atlantic Forest remnant, a relevant Brazilian biome. Additionally, different smoothing filters for the CHM surfaces were tested and the implications for the accuracy in tree determination were evaluated.

MATERIAL AND METHODS

Description of the área

The study was conducted in a forest fragment called "Capão da Engenharia Florestal" (Figure 1), located at the Federal University of Paraná, in Jardim Botânico, Campus III, Brazil. According to Machado et al. (2008), the area contains approximately 15.24 hectares, of which 12.96 hectares are Mixed Ombrophylous Forest (MOF) and the remaining area (about 2.28 hectares) is stocked with other forest formations (Neto et al., 2002).

The area has a mesothermal humid subtropical climate with cool summers and winters with frequent frosts. The region's climate is Cfb according to the Köppen climate classification, with average annual temperature and precipitation of approximately 17 °C and 1,400 mm, respectively (Alvares et al., 2013) with an average altitude of 900 meters (Machado et al., 2013).

Remotely Sensing Data

The first step to collect remotely sensing data was flight planning, considering flight planning applications and flight designs. For this purpose, two software programs were selected: Litchi (Litchi, 2022) and Pix4Dcapture (Pix4D, 2022). The flights were performed with single and double flight arrangements (Figure 2). Thus, the planning totaled eight flights, four for each evaluated application. The general parameters of each flight are shown in Table 1, with the only fixed parameters being flight height (120 m) and flight speed (8 m/s).

The flights were performed using a Phantom 4 Pro Remotely Piloted Aircraft (RPA) from the DJI brand, equipped with a FC 6310 camera and RGB sensor, with a resolution of 5472 x 3648 pixels, 20 MP (megapixels), 84° Field of View, focal length of 8.8 mm/24 mm, and 1" CMOS (Complementary Metal-Oxide Semiconductor) sensor (DJI, 2022). The flights were conducted in the research area in July 2022, during the day (10 am and 4 pm).

Ground Control Points were not used due to the characteristics of the area, especially since it is a native forest remnant and due to access difficulties, and for not being interested in the positional quality of arboreal individuals, as they emerge from the canopy and are easy to view.

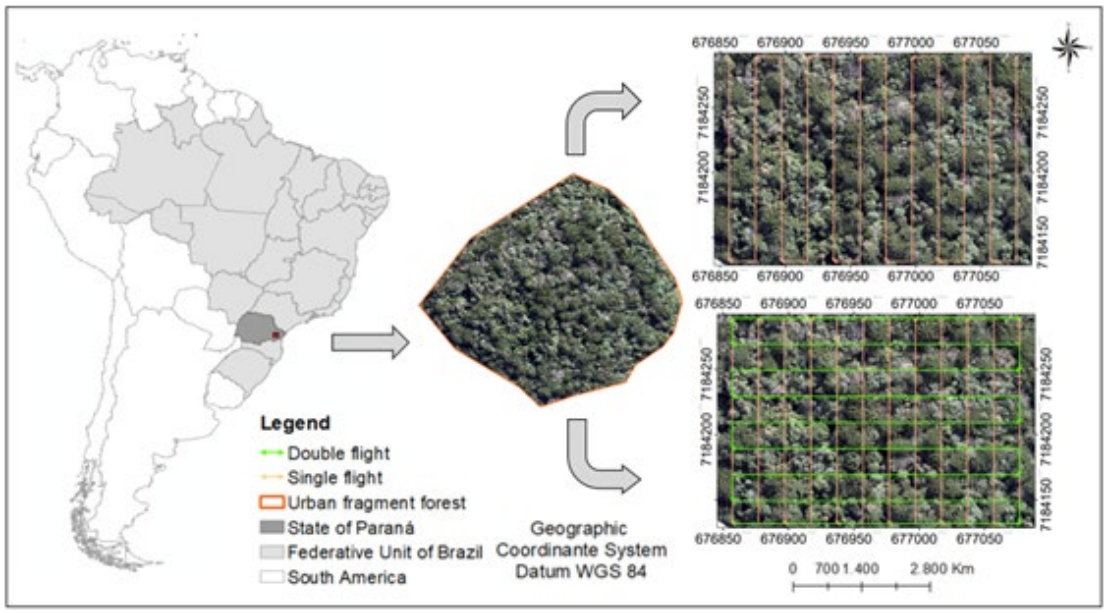

Figure 1: Study area located in the state of Paraná, Brazil.

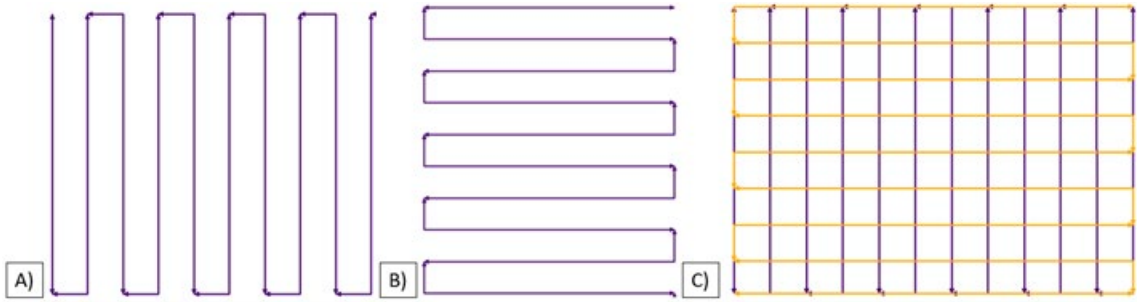

Figure 2: Flight pattern for A) North and South Serpentine and B) East and West Serpentine and C) Crosshatch Serpentine for single and double flights.

Table 1: Flight planning in Litchi and Pix4Dcapture software programs.

Parameter	DF1	DF2	SF1	SF2
Speed (m/s)	8	8	8	8
Height (m)	120	120	120	120
Distance between lines (m)	51	33	33	25
Theoretical GSD (cm)	3.16	3.16	3.16	3.16
Side overlap (%)	70	80	80	85
Longitudinal overlap (%)	70	80	80	85

Which: DF1: double flight 1; DF2: double flight 2; SF1: single flight 1; SF2: single flight 2.

In the Pix4Dmapper software (Pix4D, 2022), the initial processing involved positioning and aligning the photos obtained in the field and their adjustment by the Structure from Motion (SfM) algorithm (Jiang et al., 2020). This algorithm performs a combination of images with each other based on characteristic points, marked in at least two images (Śledź and Ewertowski, 2022). As a result, a sparse point cloud is initially obtained and subsequently a dense cloud, which in turn is the basis for generating the final photogrammetric products and identifying the homologous points to obtain the superimposition of the images collected. In this process, the point cloud is constructed, and the orthomosaic and DSM are created using noise reduction filters and the IDW statistical interpolator.

LiDAR (Light Detection and Ranging) data collection was performed with the DJI Matrice 300 system, L1 sensor, on 10/11/2021. The data were subsequently processed using the rLiDAR (Silva et al., 2017) and lidR (Roussel et al., 2020) packages in the R software (R Core Team, 2022) to derive a Digital Terrain Model (DTM), using the function grid terrain. This function creates a rasterized surface representing the terrain by interpolating the ground points and has several algorithms available like Triangular Irregular Network (TIN), Inverse Distance Weighting (IDW) and kriging (Mohan et al. 2021). In this study, TIN was used to derive a DTM.

The CHMs were generated for each flight performed, from the DSM resulting from the UAV survey under the conditions presented in Table 1, and the DTM obtained with the LiDAR. To detect the trees (Figure 3), the CHMs were smoothed with the CHMsmoothing function of the rLIDAR package (Silva et al., 2017), considering three different window sizes (ws) (1: 6.5 x 6.5 pixels; 2: 8 x 8 pixels; 3: 10 x 10 pixels) and two filters (gaussian and mean). To delimit the canopies, the locate_trees function from the lidR package was tested (Roussel et al., 2020) in the R software (R Core Team, 2022).

To evaluate the accuracy of individual tree identification, 465 individuals identified through a forest inventory carried out in 2021 and 2022 (Figure 4) were compared with the number of trees correctly identified (true positive TP), the omitted trees (false negative – FN) and the that were incorrectly classified (false positive - FP) were quantified to calculate evaluative metrics, such as recall (r) (Equation 1), precision (Equation 2), F-score (Equation 3), a measure of precision that determines the harmonic mean of recall and detection precision (Adnan et al., 2021).

$$r = \frac{TP}{TP + FN} \quad (1)$$

$$p = \frac{TP}{TP + FP} \quad (2)$$

$$F = \frac{2 * r * p}{r + p} \quad (3)$$

The design was completely randomized with three treatments (detection resulting from data without smoothing, detection resulting from data smoothed with a Gaussian filter and detection resulting from data smoothed with a mean filter). Analysis of Variance (ANOVA) was performed to evaluate the significance between the methods and verify whether there are significant differences between the tested methods. If positive, the Tukey means test will be applied. The analyzes were carried out using the R software version 4.2.0 (R CORE TEAM, 2022).

RESULTS

The implementation of different flight parameters and the application of smoothing effects on the CHMs obtained resulted in underestimates of the number of individuals. Among the three search window sizes tested, the window size of size 10 in the double flight with 80% lateral and longitudinal overlap performed in Litchi presented the lowest number of trees detected.

Combinations between CHMs without smoothing and different search window sizes do not result in accurate detections of all trees. When analyzing only the data that was not smoothed, the smoothing window of size 8 resulted in the values with the statistical metrics highest: recall, precision and F-score (Table 2). In this parameter, in the smaller search window (window size 6.5), the number of falsely detected trees was greater and with the increase in window size (10), there was a greater omission of trees.

In the best smoothing window (window size of 8), the highest F-score was 0.94 in single flight 1 run with the Litchi application. Next, we highlight the double flight 1 conducted with Pix4D with an F-score of 0.91 and with 89 individuals who were not identified.

The smoothing of the CHMs using the Gaussian filter with three search windows detected between 121 and 423 trees with F-scores between 0.43 and 0.93. Again, the average smoothing window (window size of 8) outperformed the other search filters tested. In this search window, simple flight 1 performed with Pix4D correctly detected 326 individuals, omitting 30 trees and incorrectly

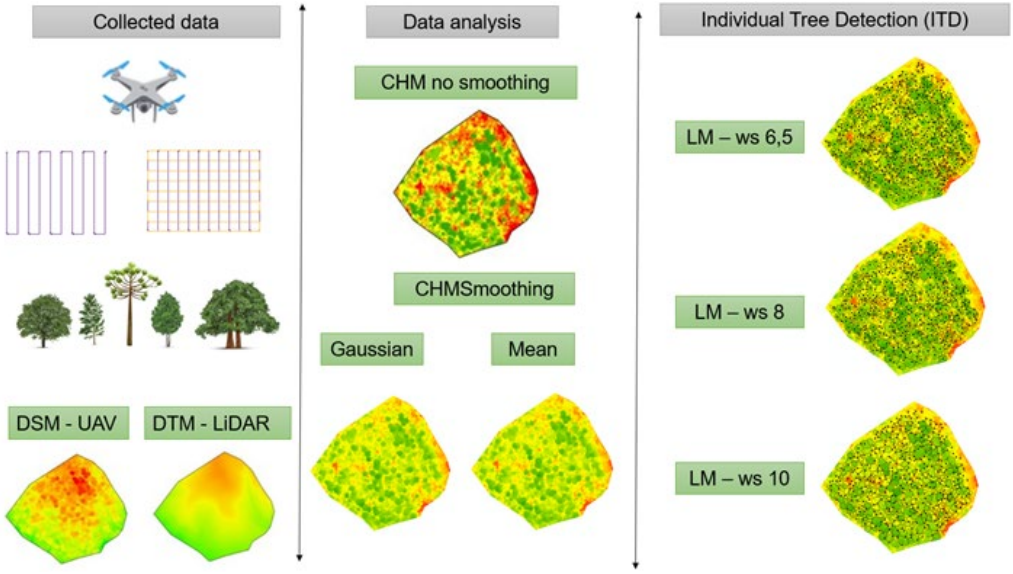

Figure 3: Tree detection overview: data collection, analyses and individual tree detection.

classifying only 18 trees (Table 3). Double flight 2 with Litchi with window size of 8 presented the lowest values of the accuracy metrics for individual tree identification.

The incorporation of the mean filter in different search sizes of individuals did not result in gains in the detection of individuals. The search filter with size 8 generated the best results, with two flights performed with Pix4D standing out from the others, with an F-score of 0.89, for double flight 2 and single flight 1, respectively (Table 4).

Statistical analysis showed that there was no significant difference between the accuracy of detecting trees without smoothing and applying filters for detection (Table 5).

Figure 5 compares the tested approaches, highlighting the differences between each method.

After planning the flights based on the assigned parameters and executing them under the observed conditions, we found that the potential GSD obtained was higher than the planned GSD for all flights, with flights performed with Litchi having a GSD of 3.27 cm and flights performed with Pix4D having, on average, 3.20 cm. Still regarding the intrinsic parameters of the flight, the average density of points per square meter ranged from 67.39 to 81.95 pts.m^{-2} for Litchi and from 68.17 to 91.57 pts.m^{-2} for Pix4D.

Figure 4: Example of manual tree detection based on orthomosaics and CHMs.

Table 2: Results of the ITD approach in the Brazilian Atlantic Forest Remnant using different flight parameters and smoothing window size considering only the CHMs.

F	WS	NT	TP	FN	FP	R	P	F	NT	TP	FN	FP	R	P	F
DF1	6.5	465	364	164	45	0.69	0.89	0.78	461	267	199	63	0.57	0.81	0.67
DF2	6.5	462	299	261	81	0.53	0.79	0.64	460	245	260	58	0.49	0.81	0.61
SF1	6.5	462	254	288	70	0.47	0.78	0.59	462	227	225	53	0.50	0.81	0.62
SF2	6.5	462	230	287	62	0.44	0.79	0.57	462	208	235	42	0.47	0.83	0.60
DF1	8	465	315	150	69	0.68	0.82	0.74	460	350	47	26	0.88	0.93	0.91
DF2	8	460	340	86	33	0.80	0.91	0.85	461	334	55	28	0.86	0.92	0.89
SF1	8	460	378	28	22	0.93	0.95	0.94	461	304	106	30	0.74	0.91	0.82
SF2	8	460	318	87	24	0.79	0.93	0.85	462	301	107	26	0.74	0.92	0.82
DF1	10	465	105	329	18	0.24	0.85	0.38	462	139	179	27	0.44	0.84	0.57
DF2	10	462	96	245	23	0.28	0.81	0.42	462	118	203	25	0.37	0.83	0.51
SF1	10	462	106	226	17	0.32	0.86	0.47	461	120	213	27	0.36	0.82	0.50
SF2	10	463	107	233	24	0.31	0.82	0.45	460	125	222	22	0.36	0.85	0.51

Which: F: flight; WS: window size; DF1: double flight 1; DF2: double flight 2; SF1: single flight 1; SF2: single flight 2; NT: number of trees; TP: true positive; FN: falses negatives; FP: falses positives; R: recall; P: precision; F: F-score.

Table 3: ITD approach for tree detection using different flight parameters and smoothing window size with gaussian filter.

F	WS	NT	TP	FN	FP	R	P	F	NT	TP	FN	FP	R	P	F
DF1	462	237	305	66	0.44	0.78	0.56	462	199	292	66	0.41	0.75	0.53	462
DF2	460	218	308	80	0.41	0.73	0.53	461	211	295	28	0.42	0.88	0.57	460
SF1	461	264	244	44	0.52	0.86	0.65	460	251	249	37	0.5	0.87	0.64	461
SF2	460	244	301	37	0.45	0.87	0.59	461	207	213	31	0.49	0.87	0.63	460
DF1	460	353	71	21	0.83	0.94	0.88	460	272	141	25	0.66	0.92	0.77	460
DF2	460	236	176	45	0.57	0.84	0.68	461	343	44	28	0.89	0.92	0.91	460
SF1	462	369	43	20	0.9	0.95	0.92	460	326	30	18	0.92	0.95	0.93	462
SF2	463	362	38	61	0.91	0.86	0.88	462	293	102	15	0.74	0.95	0.83	463
DF1	461	92	105	37	0.47	0.71	0.56	460	134	180	25	0.43	0.84	0.57	461
DF2	462	99	239	22	0.29	0.82	0.43	460	111	205	25	0.35	0.82	0.49	462
SF1	460	139	188	26	0.43	0.84	0.57	462	119	294	27	0.29	0.82	0.43	460
SF2	461	106	232	24	0.31	0.82	0.45	460	129	176	20	0.42	0.87	0.57	461

Which: F: flight; WS: window size; DF1: double flight 1; DF2: double flight 2; SF1: single flight 1; SF2: single flight 2; NT: number of trees; TP: true positive; FN: falses negatives; FP: falses positives; R: recall; P: precision; F: F-score.

Table 4: Tree detection using ITD approach with different flight parameters and smoothing window size with mean filter.

F	WS	NT	TP	FN	FP	R	P	F	NT	TP	FN	FP	R	P	F
DF1	6.5	462	223	322	76	0.41	0.75	0.53	461	152	325	110	0.32	0.58	0.41
DF2	6.5	460	213	339	84	0.39	0.72	0.50	461	218	304	36	0.42	0.86	0.56
SF1	6.5	461	245	275	41	0.47	0.86	0.61	460	195	325	47	0.38	0.81	0.51
SF2	6.5	462	188	356	72	0.35	0.72	0.47	462	214	314	29	0.41	0.88	0.56
DF1	8	460	364	84	41	0.81	0.90	0.85	460	364	84	41	0.81	0.90	0.85
DF2	8	461	339	142	69	0.70	0.83	0.76	461	339	142	69	0.70	0.83	0.76
SF1	8	462	314	102	27	0.75	0.92	0.83	462	314	102	27	0.75	0.92	0.83
SF2	8	461	342	70	33	0.83	0.91	0.87	461	342	70	33	0.83	0.91	0.87
DF1	10	462	100	220	17	0.31	0.85	0.46	461	132	182	27	0.42	0.83	0.56
DF2	10	463	94	235	23	0.29	0.80	0.42	460	115	199	28	0.37	0.80	0.50
SF1	10	462	139	188	26	0.43	0.84	0.57	462	122	207	26	0.37	0.82	0.51
SF2	10	461	107	236	24	0.31	0.82	0.45	461	125	219	23	0.36	0.84	0.51

Which: F: flight; WS: window size; DF1: double flight 1; DF2: double flight 2; SF1: single flight 1; SF2: single flight 2; NT: number of trees; TP: true positive; FN: falses negatives; FP: falses positives; R: recall; P: precision; F: F-score.

Table 5: Analysis of Variance (ANOVA) results for treatments considering applications (Litchi and Pix4D) and flight designs (single and double flight).

Litchi					
Source of Variation	**DF**	**SS**	**MS**	**F-value**	**p-value**
Trat	2	0.0007	0.0038	0.1228	0.8848
Residuals	33	1.0239	0.0310	-	-
Pix4D					
Source of Variation	**DF**	**SS**	**MS**	**F-value**	**p-value**
Trat	2	0.0150	0.0075	0.2940	0.7472
Residuals	33	0.8445	0.0255	-	-
Single flight					
Source of Variation	**DF**	**SS**	**MS**	**F-value**	**p-value**
Trat	2	0.0124	0.0062	0.2143	0.8082
Residuals	33	0.9577	0.0290	-	-
Double flight					
Source of Variation	**DF**	**SS**	**MS**	**F-value**	**p-value**
Trat	2	0.0318	0.0159	0.5992	0.5551
Residuals	33	0.8770	0.0265	-	-

Which: Trat: treatment; DF: degree of freedom; SS: Sum of Squares; MS: Mean Square.

The DSMs derived from Litchi flights had an average altitude of 51.08 meters and 52.04 meters for Pix4D. The variation in the heights of the CHMs used was also similar between the applications and arrangements tested, being slightly higher for Litchi, at 30.62 meters for Litchi and 29.92 meters for Pix4D (Figure 6).

DISCUSSION

In view of the results obtained, it can be seen that the planned GSD differed from the potential GSD (Ground Sample Distance) for each orthomosaic obtained under the studied conditions. This is due to the digital processing techniques employed which were mostly simple and used data in its raw form. Thus, it is worth highlighting the importance of using robust methods of digital image processing to produce higher quality and more accurate information. In this sense, new methods for estimating GSD values have been developed, such as the Convolutional Neural Network (CNN) (Lee and Sull, 2019). From an input image, the CNN network performs feature extraction and a binomial tree layer. Then, the GSD value is predicted based on these extracted features, and represented by a floating-point number with exponent. The authors point out that in a database composed of eight public datasets of remote sensing images with different GSDs, the GSD prediction error rate reduced by about 25% compared to a baseline network which directly estimates the GSD using the network developed.

Drag was noted in the flight arrangements tested, but with a greater incidence in dual arrangements and with greater overlap. Another important factor was the flight time, as flights carried out in the afternoon had a higher incidence of wind and, consequently, greater drag in the images. It is known that drag is a consequence of flight speed, exposure time, focal length and flight height. In this research, the flight speed was pre-established at 8 m.s in planning and varied approximately ±2 m/s during the execution of the aerial survey due to the tested application and wind conditions.

Furthermore, UAV flight trajectories planned with various configurations and flight software combined with LiDAR data were influenced by the conditions of the evaluated forest. The canopy with a high density of individuals formed by emerging canopies interfered with the number of points on the ground identified by the LiDAR sensor and the generation of the DTM accurately (Moe et al., 2020) and consequently, the extraction of CHMs, which in turn, were the inputs for tree detection.

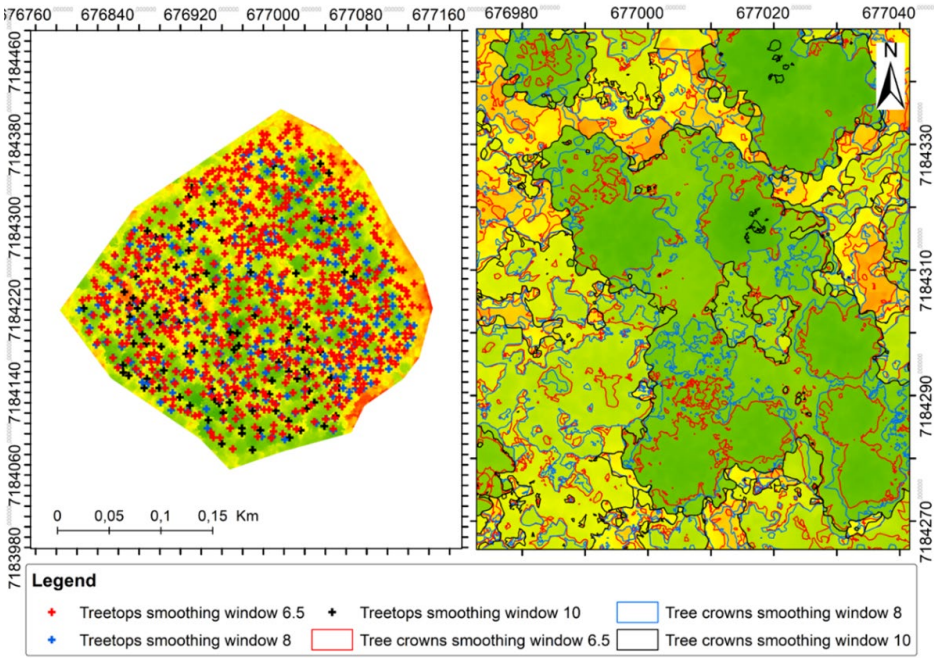

Figure 5: Results of the ITD approach applied to native trees in Native Brazilian Atlantic Forest Remnant.

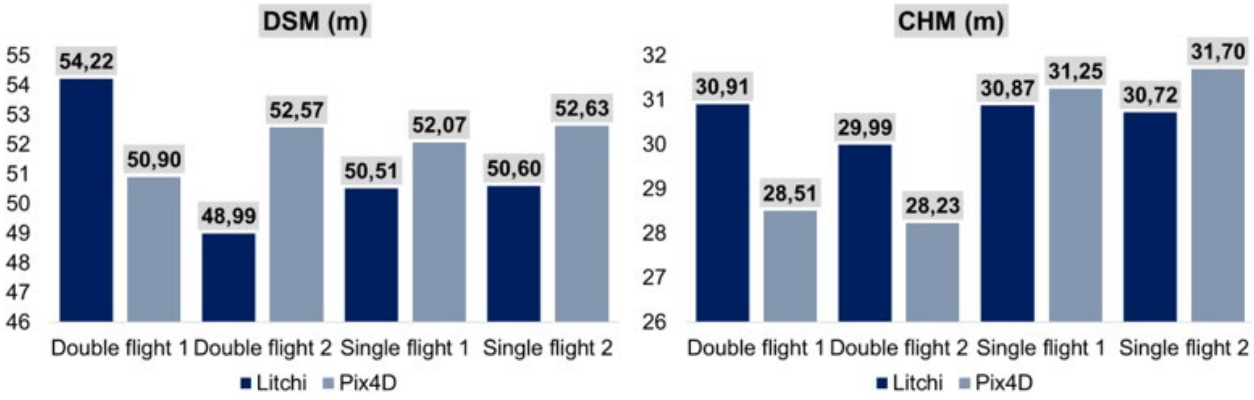

Figure 6: Comparison of digital models (DSM and CHM) obtained from different UAV flight configurations and LiDAR data.

Still in this context, it is worth highlighting that the Remote Sensing technologies used (UAVs and UAV-Lidar) have different modes of acquisition, resolution and data production. The combination of these data was tested in the same native fragment evaluated in this research, estimating tree heights with RMSE (%) of 6.38 and 12.83%, respectively. When using data generated only with UAV, the RMSE (%) increased to 49.91% (Cunha Neto et al., 2023).

Another influencing factor refers to the age of the trees present in this native fragment. Machado et al. (2008) reported the existence of trees older than 100 years. This fact, combined with the large number of trees, limited their detection and, consequently, the delimitation of their crowns. In young forests, in turn, the research carried out by Gülci (2019) and Moe et al. (2020) were satisfactory in detecting and identifying tree crowns with UAV images. Still in this context, Ottoy et al. (2022) identified Taxus spp. and olive trees in Greece with F-scores ranging from 0.88 to 0.99 with smoothing techniques and 3 x 3 pixels search windows.

As it is a native fragment with a dense canopy, the smoothing methods of the CHMs generated from the rLiDAR package (Silva et al., 2017) may have been influenced by the quality of the LiDAR data acquired, its processing and/or post -processing beyond forest conditions (Douss and Farah, 2022).

Individual tree detection from CHM requires a high-resolution model that faithfully represents the upper layer of the forest canopy (Khosravipour et al., 2016). Therefore, CHM cell size is a key parameter in detection, as cell size cannot be larger than half the size of the tree crown according to Nyquist sampling theory (Mielcarek et al., 2018). Therefore, it is recommended to apply approaches based on smoothing filters, such as mean, median or Gaussian, to reduce the occurrence of problems in the CHM.

Thus, the different flight conditions resulted in DSMs with different elevations among the applications tested, and consequently in CHMs with different heights. This factor has a great impact on ITD performance, as the LM algorithm is mainly based on the tree crowns with the pixels with the highest height values in the CHMs to identify the trees using a window of varying size (Yu et al., 2022).

For the LM algorithm to work, the appropriate window size is a critical factor that affects the accuracy of tree canopy detection (Mohan et al., 2019), as the variable search window size can be determined by a relationship between canopy radius and height (Yin and Wang, 2019), by local slope break (Douss and Farah, 2020) or a mean semivariance range (Wulder et al., 2000).

In this way, the different search window sizes tested responded to the smoothing of the models in different ways, because, by increasing the search radius, the number of omitted trees (false negative) increased. This is due to the great density of individuals, in addition to the different sizes and shapes of the canopy, present in native forests. With a smaller search window, more trees were misidentified, as there were several trees in the window and because of existing similar canopy patterns, which have already been responsible for misinterpretations in other studies (Seifert et al., 2019). Therefore, the influence of different crown sizes on the detection of individual trees in classical methods (Wagner et al., 2018), such as the LM algorithm, is noted.

Smoothing techniques can reduce false positive detections, since the pixels of some individual canopies are not homogeneous in high spatial resolution images (Aeberli et al., 2021). The results indicated that, in the smoothed CHMs, the F-scores were lower than the CHMs that were not subjected to this process, as the different shapes of the canopies caused confusion in the delimitation of each individual, in addition to the structural changes caused by exposure to the wind, resulting in problems in aligning individual images (Wierzbicki et al., 2015) during the processing of UAV data.

Land topography can also be related to the quality of ITD results. As the study site has a steep slope, height normalization may have been performed with points lower or higher than the base of the tree trunk (Breidenbach et al., 2008), causing distortions in the CHM and tree canopy, forming locations with erroneous height values (Khosravipour et al., 2014).

It is worth highlighting the limitations of LM in detecting individual tree crowns in dense forests, according to Zhen et al. (2016) and Belcore et al. (2020). In these cases, Mohan et al. (2017) recommends the individual delineation of tree species for the subsequent application of classical methods of individual tree detection. Deep learning methods are also recommended for extracting information from the spatial relationship of pixels, which provides information about the textures and shapes of trees (Onishi and Ise, 2021).

As examples of these approaches, there is the artificial vision system for identifying and mapping trees using RGB images obtained by UAV and a convolutional neural network (CNN) developed by Onishi and Ise (2021), classifying seven classes of trees with more than 90% accuracy with guided gradient-weighted class activation mapping (Guided Grad-CAM) (Onishi and Ise, 2021) and the integration of LM techniques, marker-controlled watershed segmentation (MCWS), and convolutional neural networks based on mask region (Mask R-CNN) for canopy detection in young forest by Yu et al. (2022). The Mask R-CNN model with the multiband combination achieved the best accuracy with an F of 94.68%.

CONCLUSION

It is concluded in this study that the tested overlaps (70, 80 and 85%) did not present significant changes in terms of identified trees. Likewise, the two apps tested also did not result in major changes in terms of the number of individuals located.

Regarding flight designs, it was expected that tandem flights could enhance improvements in tree identification, a fact that did not occur in this work. It is concluded that in dense areas of the Atlantic Forest, the doubles caused dragging in the orthophoto, which resulted in difficulty in adequately portraying the number of trees in the forest.

Applying the mean filter resulted in the largest number of false positives (533 trees in the Litchi application and 496 trees in Pix4D). When analyzing the search window size, the smaller size caused a greater number of falsely detected trees. The larger search window resulted in a higher number of omitted trees. .

According to the results and evaluation criteria presented, the combination of a simple design, with lateral and longitudinal overlap of 80% in Litchi application provided the best tree detection with an F-score of 0.94.

AUTHORSHIP CONTRIBUTION

Project Idea: C.T.P, K.M.A.G, D.M.C.L.S, A.P.D.C

Funding: C.T.P, K.M.A.G, D.M.C.L.S, A.P.D.C

Database: C.T.P, K.M.A.G, D.M.C.L.S, H.F.P.V, A.P.D.C

Processing: C.T.P, K.M.A.G, D.M.C.L.S, H.F.P.V

Analysis: C.T.P, K.M.A.G, D.M.C.L.S

Writing: C.T.P, K.M.A.G, D.M.C.L.S, M.M, A.P.D.C

Review: M.M, A.B, C.R.S, A.P.D.C

ACKNOWLEDGEMENT

This study was financed in part by the Coordenação de Aperfeiçoamento de Pessoal de Nível Superior – Brasil (CAPES) – Finance Code 001".

REFERENCES

ADNAN, M.; HABIB, A.; ASHRAF, J.; et al. Predicting at-risk students at different percentages of course length for early intervention using machine learning models. Ieee Access, v. 9, p. 7519-7539, 2021.

AEBERLI, A.; JOHANSEN, K.; ROBSON, A.; et al. Detection of banana plants using multi-temporal multi-spectral UAV imagery. Remote Sensing, v. 13, n. 11, p. 2123, 2021.

ALVARES, C. A.; STAPE, J. L.; SENTELHAS, P. C.; et al. Köppen's climate classification map for Brazil. Meteorologische Zeitschrift, v. 22, n. 6, p. 711–728, 2013.

BREIDENBACH, J.; KOCH, B.; KÄNDLER, G.; et al. Quantifying the influence of slope, aspect, crown shape and stem density on the estimation of tree height at plot level using lidar and InSAR data. International of Journal of Remote Sensing, v. 29, n.5, p. 1511-1536, 2008.

BELCORE, E.; WAWRZASZEK, A.; WOZNIAK, E.; et al. Individual tree detection from UAV imagery using hölder exponent. Remote Sensing, v. 12, n. 15, p. 2407, 2020.

CUNHA NETO, E. M. da.; VERAS, H. F. P.; BERTI, A. L.; et al. Combining ALS and UAV to derive the height of *Araucaria angustifolia* in the Brazilian Atlantic Rain Forest. Anais da Academia Brasileira de Ciências, v. 95, n. 1, e20201503, 2023.

DJI. *Phantom 4 Pro V2.0*. 2022 a. Available at: https://www.dji.com/br/phantom-4-pro-v2. Accessed in: July 10th 2022.

DJI. *Phantom 4 Pro V2.0*. 2022 b. Available at: https://www.pix4d.com/product/pix4dmapper-photogrammetry-software. Accessed in: July 10th 2022.

DOUSS, R.; FARAH, I. R. Extraction of individual trees based on Canopy Height Model to monitor the state of the forest. Trees, Forests and People, v. 8, p. 100257, 2022.

FASSNACHT, F.E.; WHITE, J.C.; WULDER, M.A.; NÆSSET, E. Remote sensing in forestry: current challenges, considerations and directions. Forestry: An International Journal of Forest Research, v. 97, n.1, p. 11-37, 2023.

FRASER, B. T.; CONGALTON, R. G. Issues in Unmanned Aerial Systems (UAS) data collection of complex forest environments. Remote Sensing, v.10, n.6, 908, p. 1–21, 2018.

GÜLCI, S. The determination of some stand parameters using SfM-based spatial 3D point cloud in forestry studies: An analysis of data production in pure coniferous young forest stands. Environmental Monitoring and Assessment, v. 191, n. 495, 2019.

JAAFAR, W. S. W. M.; WOODHOUSE, I. H.; SILVA, C. A.; et al. Improving individual tree crown delineation and attributes estimation of tropical forests using airborne LiDAR data. Forests, v. 9, n. 12, p. 759, 2018.

JIANG, S. JIANG, C.; JIANG, W. Efficient structure from motion for large-scale UAV images: A review and a comparison of SfM tools. ISPRS Journal of Photogrammetry and Remote Sensing, v. 167, p. 230-251, 2020.

KHOSRAVIPOUR, A.; SKIDMORE, A. K.; ISENBURG, M. Generating spike-free digital surface models using LiDAR raw point clouds: A new approach for forestry applications. International Journal of Applied Earth Observation and Geoinformation, v. 52, p. 104-114, 2016.

KHOSRAVIPOUR, A.; SKIDMORE, A.K.; ISENBURG, M.; et al. Generating Pit-free Canopy Height Models from Airborne Lidar. Photogrammetric Engineering & Remote Sensing, n. 9, p. 863-872, 2014.

IGLHAULT, J.; CABO, C.; PULITI, S.; et al. Structure from Motion Photogrammetry in Forestry: a Review. Currently Forestry Reports, v.5, p. 155–168, 2019.

LEE, J. H.; SULL, S. Regression tree CNN for estimation of ground sampling distance based on floating-point representation. Remote Sensing**,** v. 11, n. 19, p. 2276, 2019.

LITCHI. *Litchi mission hub*. 2022. Available at: https://flylitchi.com/hub. Accessed in: July 15th 2022.

MACHADO, S. A.; ZAMIN, N. T.; NASCIMENTO, R. G. M et al. Comparação dos parâmetros fitossociológicos entre três estratos de um fragmento de floresta ombrófila mista. Cerne, v. 19, n. 3, p. 365–372, 2013.

MACHADO, S. A; NASCIMENTO, R. G. M.; AUGUSTYNCZIK, A. L. D.; et al. Comportamento da relação hipsométrica de Araucaria angustifolia no capão da Engenharia Florestal da UFPR. Pesquisa Florestal Brasileira, n. 56, p.5-16, 2008.

MIELCAREK, A.; STEREŃCZAK, K.; KHOSRAVIPOUR, A. Testing and evaluating different LiDAR-derived canopy height model generation methods for tree height estimation. International Journal of Applied Earth Observation and Geoinformation, v. 71, p. 132-143, 2018.

MILLIKAN, P. H. K.; SILVA, C. A; RODRIGUEZ, L. C. E.; et al. Automated individual tree detection in amazon tropical forest from airborne laser scanning data. Cerne, v. 25, n. 3, p.273-282, 2019.

MOHAN, M.; LEITE, R. V.; BROADBENT, E. N.; et al. Individual tree detection using UAV-lidar and UAV-SfM data: A tutorial for beginners. Open Geosciences, v. 13, n. 1, p. 1028-1039, 2021.

MOHAN, M.; MENDONÇA, B. A. F.de.; SILVA, C. A.; et al. Optimizing individual tree detection accuracy and measuring forest uniformity in coconut (*Cocos nucifera* L.) plantations using airborne laser scanning. Ecological Modelling, v. 409, p. 108736, 2019.

MOHAN, M.; SILVA, C. A.; KLAUBERG, C.; et al. Individual tree detection from unmanned aerial vehicle (UAV) derived canopy height model in an open canopy mixed conifer forest. Forests**,** v. 8, n. 9, p. 340, 2017.

MOHSAN, S. A. H.; KHAN, M. A.; NOOR, F.; et al. Towards the unmanned aerial vehicles (UAVs): A comprehensive review. Drones, v. 6, n. 6, p.147, 2022.

MOE, K. T.; OWARI, T.; FURUYA, N.; et al. Comparing Individual Tree Height Information Derived from Field Surveys, LiDAR and UAV-DAP for High-Value Timber Species in Northern Japan. Forests**,** v. 11, n. 2, p. 223, 2020.

NEVALAINEN, O.; HONKAVAARA, E.; TUOMINEN, S.; et al. Individual Tree Detection and Classification with UAV-Based Photogrammetric Point Clouds and Hyperspectral Imaging. Remote Sensing, v. 9, n. 3, p. 185, 2017.

NETO, R. M. R.; KOZERA, C.; ANDRADE, R. D. R. de.; et al. Caracterização florística e estrutural de um fragmento de Floresta Ombrófila Mista, em Curitiba, PR–Brasil. Floresta, v. 32, n. 1, p. 3-16, 2002.

ONISHI, M; ISE, T. Explainable identification and mapping of trees using UAV RGB image and deep learning. Scientific Reports, v. 11, n. 1, p. 903, 2021.

OTTOY, S.; TZIOLAS, N.; MEERBEEK, K. V.; et al. Effects of Flight and Smoothing Parameters on the Detection of Taxus and Olive Trees with UAV-Borne Imagery. Drones, v. 6, n. 8, p. 197, 2022.

Pix4D. *Pix4Dcapture*. 2022a. Available at: https://www.pix4d.com/product/pix4dcapture. Accessed in: July 15th 2022.

R Core Team. 2022 R: A language and environment for statistical computing. R Foundation for Statistical Computing, Vienna, Austria.

ROUSSEL, J-R.; AUTY, D.; COOPS, N. C.; et al. lidR: An R package for analysis of Airborne Laser Scanning (ALS) data. Remote Sensing of Environment, v. 251, p. 112061, 2020.

SEIFERT, E.; SEIFERT, S.; VOGT, H.; et al. Influence of drone altitude, image overlap, and optical sensor resolution on multi-view reconstruction of forest images. Remote sensing, v. 11, n. 10, p. 1252, 2019.

SILVA, C. A.; CROOKSTON, N. L.; HUDAK, A.T.; et al. rLiDAR: LiDAR Data Processing and Visualization. 2017.

ŚLEDŹ, S; EWERTOWSKI, M. W. Evaluation of the Influence of Processing Parameters in Structure-from-Motion Software on the Quality of Digital Elevation Models and Orthomosaics in the Context of Studies on Earth Surface Dynamics. Remote Sensing, v. 14, n. 6, p. 1312, 2022.

TANG, L.; SHAO, G. Drone remote sensing for forestry research and practices. Journal of Forest Research, v. 26, n.4, p. 791-797, 2015.

WAGNER, F. H.; FERREIRA, M. P.; SANCHEZ, A.; et al. Individual tree crown delineation in a highly diverse tropical forest using very high resolution satellite images. ISPRS Journal of Photogrammetry and Remote Sensing, v. 145, p. 362-377, 2018.

WIERZBICKI, D; KEDZIERSKI, M; FRYSKOWSK, A. Assesment of the influence of UAV image quality on the orthophoto production. The International Archives of the Photogrammetry, Remote Sensing and Spatial Information Sciences, v. XL-1/W4, 2015.

WULDER, M.; NIEMANN, K. O.; GOODENOUGH, D. G. Local Maximum Filtering for the Extraction of Tree Locations and Basal Area from High Spatial Resolution Imagery. Remote Sensing of Environment, v. 73, n.1, p. 103–114, 2000.

YIN, D; WANG, L. Individual mangrove tree measurement using UAV-based LiDAR data: Possibilities and challenges. Remote Sensing of Environment, v. 223, p. 34-49, 2019.

YU, K.; HAO, Z.; POST, C. J.; et al. Comparison of classical methods and mask R-CNN for automatic tree detection and mapping using UAV imagery. Remote Sensing, v. 14, n. 2, p. 295, 2022.

ZHEN, Z.; QUACKENBUSH, L. J.; ZHANG, L. Trends in automatic individual tree crown detection and delineation-evolution of LiDAR data. Remote Sensing, v. 8, n. 4, p. 333, 2016.